

Multiple melting in blends of poly(vinylidene fluoride) with isotactic poly(ethyl methacrylate)

A. Eshuis, E. Roerdink and G. Challa

Laboratory of Polymer Chemistry, State University of Groningen, Nijenborgh 16, 9747

AG Groningen, The Netherlands

(Received 23 January 1981; revised 10 April 1981)

Multiple melting phenomena have been studied in blends of poly(vinylidene fluoride) (PVF₂) with low molar mass isotactic poly(ethyl methacrylate) (it-PEMA). In all blends, as well as in pure PVF₂, a transition (T_1) was observed prior to the main melting point (T_2). T_1 is probably connected with the melting of secondarily-crystallized material. In addition to this, a high temperature melting endotherm (T_3) was observed, which could be ascribed completely to recrystallization of PVF₂. The highest transition (T_4) was caused by melting of the γ form of PVF₂. From Hoffman-Weeks plots — T_2 vs. crystallization temperature, T_c — it could be concluded that no thermodynamic depression of the melting point of PVF₂ occurred in the blends. The stabilities of PVF₂ crystallites in the various blends were derived from the slopes of Hoffman-Weeks plots and were in good agreement with lamellar thicknesses found from SAXS measurements.

Keywords Multiple melting; blends; poly(vinylidene fluoride); isotactic poly(ethyl methacrylate)

INTRODUCTION

Multiple melting has often been observed in semi-crystalline polymers. Occurrence of more than one polymorphic crystalline modification¹ and recrystallization of primarily-formed crystals into more perfect ones during differential scanning calorimetry (d.s.c.) are the most common explanations^{2,3}.

In studies of blends of PVF₂ with poly(alkyl methacrylates) multiple melting behaviour has not previously been observed, except by Roerdink and Challa^{4,5}. If the melting point depression of PVF₂ is used to find the binary Flory-Huggins interaction parameter, χ_{12} , it should be possible to assign the various melting endotherms and to make a correct estimation of this parameter.

Here, we have assigned the endotherms for blends of PVF₂ with low molar mass it-PEMA, for which interesting lower critical solution temperature (LCST) behaviour at temperatures above the melting point has been recently reported^{6,7}.

EXPERIMENTAL

The PVF₂ resin (KF polymer) was obtained in granular form from the Kureha Chemical Industry Co. Ltd and was the same as used previously⁸.

To synthesize it-PEMA with a low molar mass, equal volumes (about 40 cm³) of 2 M phenylmagnesium bromide solution in ether and ethyl methacrylate monomer were simultaneously added dropwise to about 500 cm³ distilled toluene with continuous stirring. After all reactants had been mixed (within $\frac{1}{2}$ h), the reaction was allowed to proceed for 12 h. Purification of the low molar mass it-PEMA was achieved by successive precipitations

from chloroform into n-hexane and from acetone into distilled water at 0°C. Characterization of it-PEMA and preparation of the blends was described previously⁴. Characterization data for it-PEMA in this study were as follows: $[\eta] = 4 \text{ cm}^3 \text{ g}^{-1}$, $\bar{M}_w = 3000$; triads: I = 79, H = 15, S = 6.

Melting and crystallization temperatures, T_m and T_c , were measured with a Perkin-Elmer differential scanning calorimeter (DSC-IB) at a heating rate of 8°C min⁻¹, unless otherwise stated. The maximum of a melting endotherm was taken as melting temperature.

The LCST of blends of PVF₂ with our rather low molar mass it-PEMA was observed at 183°C⁷, which is above the melting temperature of PVF₂. To avoid liquid-liquid phase separation the temperature of the blends was not raised above the LCST. We chose the low molar mass polymer because increasing the molecular weight of it-PEMA causes the LCST to shift to lower values.

Small-angle X-ray scattering (SAXS) was used to obtain information on the morphology of PVF₂ crystallized from blends with it-PEMA. Samples of different composition were allowed to crystallize at 143°C overnight. The intensity of the scattered radiation was recorded photographically with a Statton camera, scanned afterwards with a microdensitometer and stored on magnetic tape. The observed and Lorentz-corrected⁹ intensities were obtained as a function of scattering angle, using a high-speed digital computer.

RESULTS

Multiple melting is observed in blends of PVF₂ with it-PEMA (Figure 1). D.s.c. curves of a 50-50 PVF₂/it-PEMA blend isothermally-crystallized at different

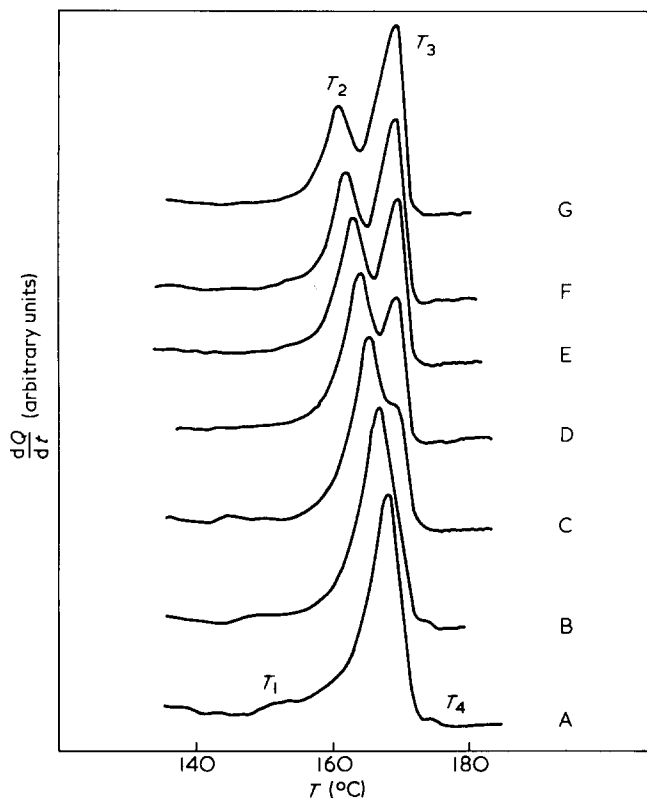


Figure 1 Thermograms of completely crystallized 50-50 PVF₂/it-PEMA blends recorded by d.s.c. at a heating rate of 8°C min⁻¹. Crystallization temperatures T_c : A, 147°C; B, 144°C; C, 141°C; D, 138°C; E, 135°C; F, 132°C; G, 129°C. After crystallization for (at most) 30 min, samples were first cooled to 100°C

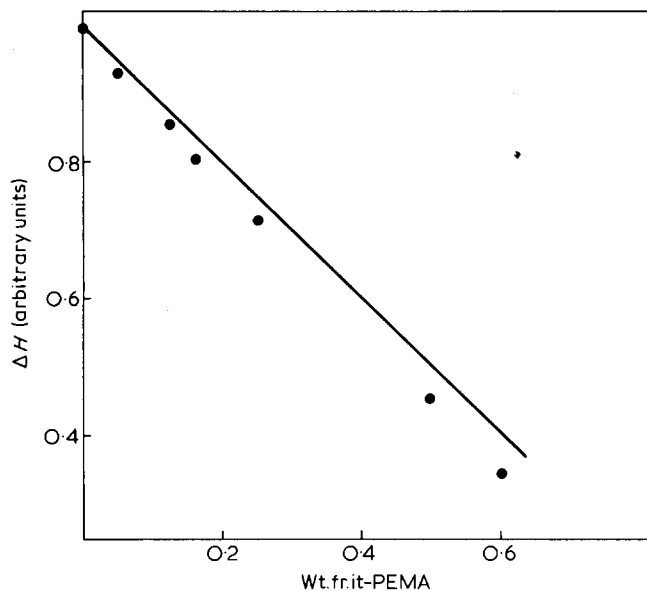


Figure 2 Endotherm area, ΔH (arbitrary units), of PVF₂/it-PEMA blends isothermally crystallized at 140°C, recorded by d.s.c. at a heating rate of 8°C min⁻¹. Full line, ΔH if it-PEMA had no effect on crystallization of PVF₂

temperatures are shown as examples. In some cases as many as four transitions can be identified. The lowest transition, T_1 , appears just above the crystallization temperature, T_c , and vanishes at lower T_c .

For higher T_c one main melting endotherm, T_2 , is observed. This gradually splits into two endotherms, T_2 and T_3 , with decreasing T_c . The former is strongly

dependent on T_c , whereas the latter is constant within experimental error. After crystallization at the highest T_c a minor transition, T_4 , is observed between 170° and 180°C.

Possible melting of crystallized it-PEMA could explain the multiple melting. To test this, heats of fusion of samples crystallized at 140°C for 24 h were measured as a function of wt% it-PEMA in the blends. From the results it can be concluded that no polymer crystallized from the blends in addition to PVF₂ (Figure 2)—otherwise ΔH should rise again for high it-PEMA contents.

To find the origin of T_3 in addition to T_2 , a double melting 50-50 PVF₂/it-PEMA sample, isothermally crystallized at 130°C, was annealed at 167°C, between the melting temperatures T_2 and T_3 . The area of the latter endotherm increased at the cost of the former. Longer annealing times at this temperature—for instance 16 h—even caused a complete 'shift' of the T_2 to the T_3 endotherm (Figure 3). Thus, it can be seen from Table 1 that at increasing d.s.c. heating rates T_3 shifts to lower

Table 1 Melting temperatures and total endotherm area ΔH of a 50-50 PVF₂/it-PEMA blend, isothermally crystallized at 130°C, as a function of heating rate in the d.s.c.

Heating rate (°C min ⁻¹)	T_2 (°C)	T_3 (°C)	ΔH (arb. units)
2	165.5	173.0	7.3
4	165.0	172.5	6.8
8	166.0	171.0	7.1
16	165.5	168.5	7.2
32	←One broad peak→		6.9

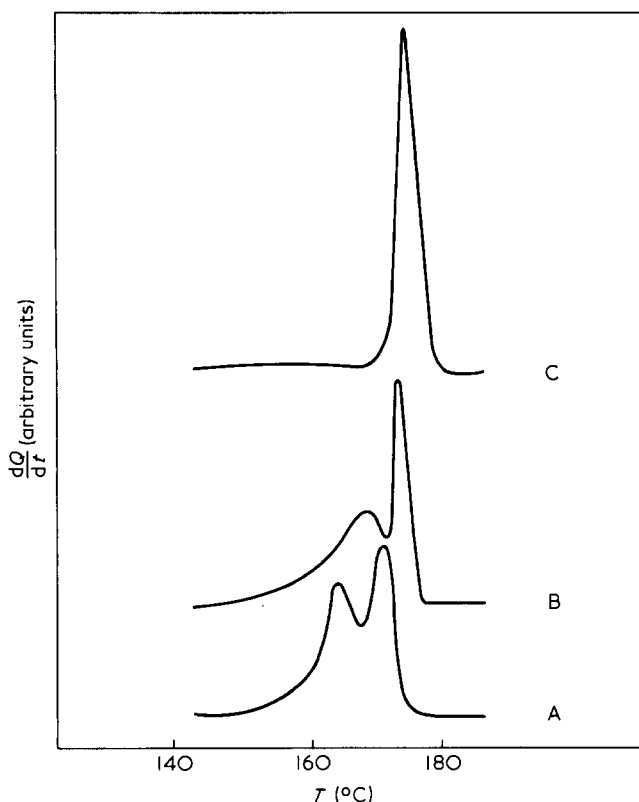


Figure 3 Thermograms of a 50-50 PVF₂/it-PEMA blend recorded by d.s.c. at a heating rate of 8°C min⁻¹; A, isothermally crystallized at 130°C; B, 2 min annealed at 167°C after crystallization at 130°C; C, 16 h annealed at 167°C after crystallization at 130°C

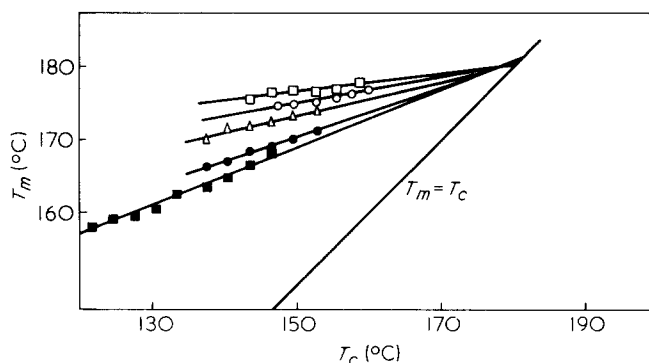


Figure 4 Hoffman-Weeks plots of melting temperatures, T_m , of pure PVF₂ and PVF₂ in blends with it-PEMA as a function of crystallization temperature, T_c . Wt ratio PVF₂/it-PEMA: ○, 100/0; □, 95/5; △, 75/25; ●, 50/50; ■, 40/60

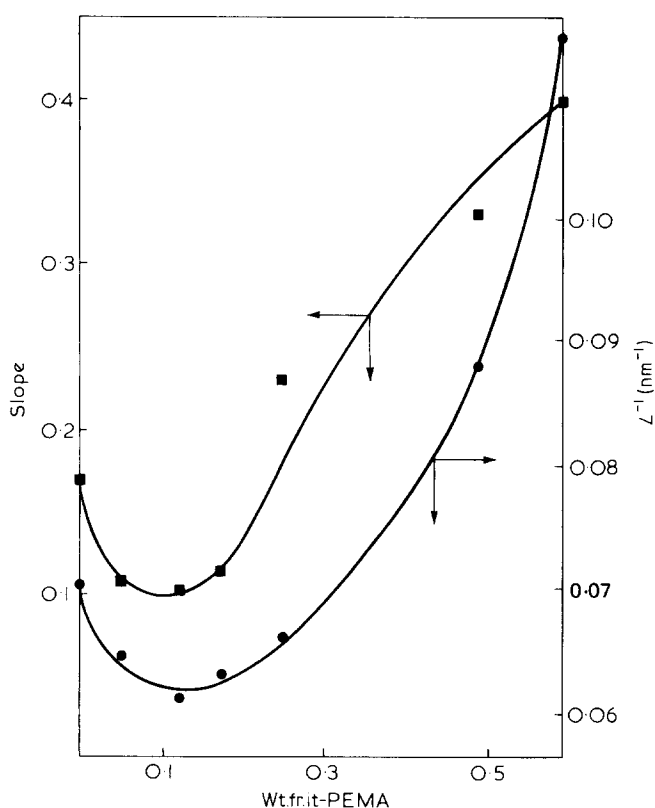


Figure 5 Slopes of T_m vs. T_c lines in Hoffman-Weeks plots and reciprocal lamellar thicknesses of various PVF₂/it-PEMA blends, as a function of it-PEMA content

temperatures, whereas T_2 remains fairly constant. This was also the case for the total heat of melting.

In Figure 4, T_2 of several PVF₂/it-PEMA blends is given as a function of T_c in Hoffman-Weeks plots. The reciprocal of the slope of the lines in this Figure, obtained by a least squares fit, is plotted against it-PEMA content in Figure 5.

The observed and Lorentz-corrected SAXS curves of pure PVF₂ are given in Figure 6. The long mean spacing, D , is obtained from the position of the maximum of the corrected curve using Bragg's law. Table 2 gives values of D for blends of PVF₂ with it-PEMA, isothermally crystallized at 143°C.

DISCUSSION

As can be seen from Figure 1, T_1 is strongly dependent on T_c , indicating an unstable type of crystallite. The same phenomena were observed by Lemstra *et al.*² for isotactic polystyrene (i-PS). These authors attributed the 'small peak just above T_c ' to the melting of secondarily-crystallized polymer in the form of intercrystalline links between lamellae of the spherulites.

The T_1 transition in PVF₂ can be observed in the d.s.c. curves in at least two papers^{3,10}, but the authors did not recognize this. T_1 occurs at temperatures too high to be the T_c transition observed by Enns and Simha at about 100°C¹¹. In our blends the T_1 transition of PVF₂ appeared more pronounced when the content of this polymer was decreased, indicating that this transition occurs as a consequence of the melting of less-perfectly crystallized material.

From Figure 2 it was concluded that it-PEMA does not crystallize from PVF₂/it-PEMA blends. For PVF₂/it-PMMA blends further evidence for such a conclusion has been obtained from X-ray patterns and infra-red spectra⁴. As it-PEMA crystallizes more slowly than it-PMMA, it is improbable that the occurrence of T_2 and T_3 in PVF₂/it-PEMA blends stems from crystallization of it-PEMA.

Because PVF₂ can exist in at least three polymorphic crystalline modifications, indicated by the α (II)-, β (I)- and

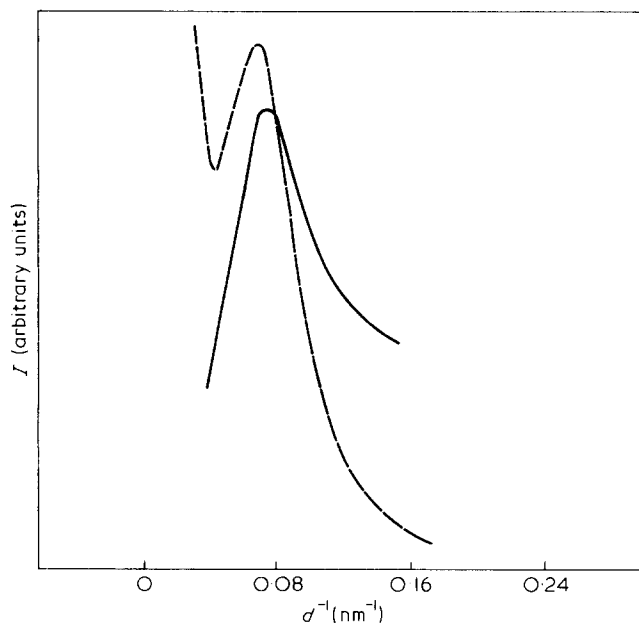


Figure 6 Observed (---) and Lorentz-corrected (—) SAXS curves for pure PVF₂

Table 2 Long mean spacing, D , of blends of PVF₂ with it-PEMA, isothermally crystallized at 143°C

Weight fraction it-PEMA	D (nm)
0	14.1
0.05	16.1
0.12	18.5
0.17	19.2
0.15	20.7
0.50	22.7
0.60	21.7

γ (III)-forms^{12,13}, occurrence of more than one of these forms had to be considered as an explanation for this complicated melting behaviour. The α -form is predominantly observed during crystallization from the melt¹⁰. The β -form is usually obtained by mechanical deformation of α -spherulites¹⁴. In the melt and at high crystallization temperatures, the higher melting γ phase is preferentially formed. The T_3 transition cannot be caused by melting of this last form because T_3 is more pronounced after crystallization at lower T_c . Instead, the T_4 transition should be assigned to the γ -form, in agreement with the results of Nakagawa and Ishida³.

Multiple melting in semicrystalline polymers often results from a melting and recrystallization process. During a d.s.c. scan the material melts, this process being followed immediately by a (partial) rearrangement into more perfect crystals. When both transformations proceed to completion there is no transition visible; when they do not there appears a peak which corresponds to the melting point, T_2 , of the primary crystal. The more perfect crystals formed in this way may melt and recrystallize again when enough time is available. Ultimately the material is no longer able to recrystallize during the scan because of decreasing undercooling, so that a final melting peak, T_3 , is observed.

Clearly the position of this peak is strongly dependent on the heating rate. Lemstra *et al.*² clearly demonstrated some features of this process for i-PS, which apply also to our results:

- (i) the independence of T_3 on T_c (Figure 1);
- (ii) the shift of T_3 to a lower value if the rate of heating is increased (Table 1);
- (iii) the independence of the total heat of fusion of both endotherms, T_2 and T_3 , and the rate of heating (Table 1);
- (iv) the 'shift' of the T_2 - to the T_3 -endotherm when the samples are annealed at an intermediate temperature (Figure 3).

Lemstra *et al.* also reported more pronounced double melting at lower scan speeds, in agreement with our results for PVF₂ blends. For pure PVF₂, however, Nakagawa and Ishida found a better resolution of the two endotherms at higher scan speeds³. These apparently contradictory results can be understood by taking into account the much higher rate of crystallization of pure PVF₂ compared with i-PS and PVF₂ blended with it-PEMA. For example, crystallization of pure PVF₂ cannot be suppressed by quenching in liquid nitrogen, whereas completely amorphous PVF₂/it-PEMA blends can be obtained by rapid cooling in a d.s.c. apparatus. At low heating rates (<5°C min⁻¹) pure PVF₂ tends to recrystallize immediately and completely after melting of the primary structure. This process goes on until recrystallization is no longer possible, resulting in one single final peak (T_3).

As the scan speed is increased, only part of the material is able to recrystallize immediately into more perfect crystals, because the average time available for recrystallization is shorter, so that two peaks are observed.

With more slowly crystallizing i-PS and PVF₂ blended with it-PEMA double melting occurs at low scan speeds, but these materials display only one peak (T_2) in a d.s.c. experiment at high scan speeds, because under these circumstances recrystallization does not occur at all.

It is now clear that in our blends T_2 is the melting

temperature of the α -modification, related to the primary crystallization process. An extrapolation of T_2 as a function of T_c to $T_2 = T_c$ in a Hoffman-Weeks plot for pure PVF₂ and for PVF₂ in blends with it-PEMA leads to the equilibrium melting temperatures of the perfect crystals, T_m^* (Figure 4)¹⁵. Within experimental error the same value for T_m^* is obtained (180°C), although the slopes of the lines vary with it-PEMA content. The slope reaches a minimum for about 10 wt % it-PEMA (Figure 5), indicating that crystallization of PVF₂ from these blends gives more stable crystallites than those formed from the pure polymer. These results can be compared with the D values obtained by SAXS measurements as given in Table 2. D is composed of the lamellar thickness of PVF₂ crystallites and the extent of the interlamellar layer of amorphous material. The average lamellar thickness l_c is related to D by¹⁶:

$$l_c = D X_c$$

where X_c is the overall degree of crystallinity. For blends we can assume:

$$X_c = x_{\text{PVF}_2} X_{c,\text{PVF}_2}$$

where x_{PVF_2} is the weight fraction PVF₂ and X_{c,PVF_2} is the degree of crystallinity of PVF₂. Thus:

$$l_c = D x_{\text{PVF}_2} X_{c,\text{PVF}_2} = L X_{c,\text{PVF}_2}$$

where $L = D x_{\text{PVF}_2}$.

Since X_{c,PVF_2} decreases only slightly with it-PEMA contents below 0.3 (Figure 2), the lamellar thickness of PVF₂ in these blends is approximately proportional to L . In Figure 5 the reciprocal of L is plotted as a function of weight fraction it-PEMA.

According to Hoffman and Weeks the slope, a , of a T_m vs. T_c plot and the lamellar thickness, l_c , are related¹⁵:

$$a = \frac{T_m^* - T_m}{T_m^* - T_c} = \frac{2\sigma_e T_m^*}{\Delta H_f (T_m^* - T_c)} \cdot \frac{1}{l_c}$$

where σ_e = surface free energy of the crystal perpendicular to the chain direction; T_m^* = equilibrium melting point; ΔH_f = heat of fusion per unit of volume; T_c = crystallization temperature.

As all samples were crystallized at the same temperature (143°C) and the other parameters are approximately constant, a and l_c^{-1} should be proportional. As can be seen from Figure 5 agreement is good over a wide range of concentrations.

To conclude, the observed melting point depressions are completely due to morphological effects and there is no thermodynamic melting point depression, i.e. $\chi_{12} = 0$.

Moreover, the melting point elevation in blends of PVF₂ with 5 wt % it-PEMA with respect to pure PVF₂ (Figure 4) can be attributed to morphological effects as well, because the minimum in the slope, a , corresponds to the maximum in the lamellar thickness (Figure 5).

ACKNOWLEDGEMENT

The authors gratefully acknowledge the help of Dr P. F. van Hutten of our Laboratory in carrying out the SAXS experiments.

REFERENCES

- 1 Jaffe, M. and Wunderlich, B. *Kolloid Z. Z. Polym.* 1967, **203**, 216–17
- 2 Lemstra, P. J., Kooistra, T. and Challa, G. *J. Polym. Sci. (A-2)* 1972, **10**, 823
- 3 Nakagawa, K. and Ishida, Y. *J. Polym. Sci., Polym. Phys. Edn.* 1973, **11**, 2153
- 4 Roerdink, E. and Challa, G. *Polymer* 1980, **21**, 509
- 5 Roerdink, E. *Thesis*, University of Groningen. Groningen (1980)
- 6 Roerdink, E. and Challa, G. *Polymer* 1980, **21**, 1161
- 7 Ten Brinke, G., Roerdink, E. and Challa, G. *MMI Press Symposium Series* Vol. 3
- 8 Roerdink, E. and Challa, G. *Polymer* 1978, **19**, 173
- 9 Crist, B. and Morosoff, N. *J. Polym. Sci., Polym. Phys. Edn.* 1973, **11**, 1023
- 10 Prest, W. M. and Luca, D. J. *J. Appl. Phys.* 1975, **46**, 4136
- 11 Enns, J. B. and Simha, R. *J. Macromol. Sci. (B)* 1977, **13**, 11
- 12 Hasegawa, R., Kobayashi, M. and Tadokoro, H. *Polym. J.* 1972, **3**, 591
- 13 Hasegawa, R., Takayashi, Y. and Tadokoro, H. *Polym. J.* 1972, **3**, 600
- 14 Prest, W. M. and Luca, D. J. *J. Appl. Phys.* 1978, **49**, 5042
- 15 Hoffman, J. D. and Weeks, J. J. *J. Res. Nat. Bur. Stand. (A)* 1962, **66**, 13
- 16 Groeninckx, G., Reynaers, H., Bergmans, H. and Smets, G. *J. Polym. Sci., Polym. Phys. Edn.* 1980, **18**, 1311